EFFECT OF GRAPHENE-GOLD NANOCOMPOSITES ON THE PHOTOCATALYTIC ACTIVITY OF TIO$_2$

VU DUC CHINH[1,†] NGUYEN THUY VAN[1], PHAM THANH BINH[1]
AND CHU THI THU HIEN[2]

[1]*Institute of Materials Science, Vietnam Academy of Science and Technology,
18 Hoang Quoc Viet, Cau Giay, Hanoi, Vietnam*

[2]*Department of Chemistry, Faculty of Building Materials, National University of Civil
Engineering, 55 Giai Phong, Hai Ba Trung, Hanoi, Vietnam*

[†]*E-mail:* chinhvd@ims.vast.vn

Abstract. *The synthesis of graphene (Gr) - gold (Au) nanoparticle (NP) composite was achieved using continuous ultraviolet wave exposure. The functional groups were investigated with FT-IR spectra. From the Raman spectra, D-band and G-band of Gr were identified. As a result, the uniform deposition of nanometer-sized Au NPs on the Gr sheets was observed from the field emission scanning electron microscope (FE-SEM) images. The photodegradation of methylene blue in aqueous solutions was studied using various photocatalysts, including neat TiO$_2$, Gr/TiO$_2$ and Gr-Au/TiO$_2$ composites. The Gr weight ratio in this research was 2% . The Gr2% -Au0.1% /TiO$_2$ composite had the highest photoactivity.*

Keywords: graphene-gold, heterogeneous composite photocatalysts, TiO$_2$..

Classification numbers: 78.67.-n; 82.50.-m; 96.30.nd.

I. INTRODUCTION

Heterogeneous photocatalysis has been appointed as a technology for the treatment of contaminated wastewater and polluted air, containing toxic or nonbiodegradable compounds [1, 2]. Among the different photocatalysts, TiO$_2$ was widely researched in numerous investigations because of its low cost, chemical stability, and lack of toxicity [3]. However, its wide band gap and the fast recombination rate of photoinduced electron-hole pairs result in the low photocatalytic efficiency limiting its practical application scopes. Graphene (Gr) incorporated with inorganic materials, in particular, metallic nanostructures (e.g. Pd, Pt, Au and Ag) [4–7] and semiconducting oxides (TiO$_2$ and ZnO) [8–10], has been appealing candidates in applications related to

many fields, catalysis, sensors, optical and electronic devices, and so forth. Metal nanoparticles (NPs) have been introduced to Gr because of their extraordinary conductivity and excellent catalytic activity [11, 12]. Thus, many approaches for the preparation of Gr-Au nanocomposite have been attempted, such as chemical reduction processes [13], physical vapor deposition [14] and hydrothermal techniques [15]. In these chemical and physical methods, Au NPs can be dispersed over Gr sheets with relatively high density and surface ratios. However, despite the large number of works in this field, up to date there is not any research governing the synthesis, characterization and photocatalytic activity of the Gr-Au/TiO$_2$ composites.

In this work, we aimed at synthesis of Gr-Au, which can use both the advantages of Gr and Au NPs to improve the photocatalytic efficiency of TiO$_2$. Herein, we report a facile route for the growth of TiO$_2$ NPs on Au/Gr sheets via sol-gel method. The materials used on the photodegradation of methylene blue (MB) dyes were in aqueous solution. A synergic role of Gr-Au loading was found to increase the photocatalytic activity of TiO$_2$. The three-component system Au0.1% –Gr2% /TiO$_2$ exhibited the highest photocatalytic activity.

II. EXPERIMENT

II.1. Materials

Gr used in this study was obtained from Laboratory of Carbon nano, Institute of Materials Science, Vietnam Academy of Science and Technology, Vietnam. Chloroauric acid with a purity of 99.999% was from Sigma-Aldrich. Tetrabutyl orthotitanate (TBOT), ethanol, and ammonia solution used in the synthesis of photocatalysts were of analytical grade (Merck, Germany) and taken without further purification.

II.2. Synthesis of Gr-Au nanocomposites

HAuCl$_4$ solution (0.01 M) was added to Gr aqueous suspension (0.3 mg/ml). The resultant suspension was sonicated during 30 min to promote the interaction of gold ions with the Gr surface. After that, the solution was then irradiated (UV lamp, 66 W) for 2 h under continuous sonicating. The resultant nanocomposite was washed with distilled water using centrifugation (12000 rpm). The final nanocomposite was dried at 80˚C overnight.

II.3. Catalyst preparation

To synthesize Gr-Au/TiO$_2$ composites, Ti(OC$_4$H$_9$)$_4$ (Merck) and Gr-Au were dissolved in ethanol solution at first, which was stirred magnetically for 30 min. Then ammonia solution (25 wt.%) was added into the solution. The mixture was loosely covered and kept stirring until a homogenous gel formed. The gel was aged in air for one day, then crushed down to fine powder and dried at room temperature. The as-prepared powder was calcined at 450˚C in a flow of nitrogen for 2 h to obtain Gr-Au/TiO$_2$ composites. For comparison purposes, neat TiO$_2$, Gr/TiO$_2$ catalysts were prepared, following exactly the above steps.

II.4. Materials characterization

Gr-Au nanocomposites were analyzed by Micro Raman spectroscopy (XploRA; Horiba) using 532 nm (90 mW) or 785 nm (25 mW) excitation radiation from a diode-pumped,

solid-state laser to .analyze the vibration bonds and their Raman frequencies. The laser power was 100 mW. Objectives of 910 were used to focus the excitation laser light on the right spot of the investigated samples. The spot size of laser beam was 1 μm. The spectral resolution was 2 cm^{-1}. The acquisition time ranged from 30 s to 120 s, but normally was 30 s. The system uses a charge coupled device (CCD) receiver with four gratings, 600 g/mm, 1200 g/mm, 1800 g/mm and 2400 g/mm, measuring from 100 cm^{-1} to 4000 cm^{-1}. Fourier transform infrared (FTIR) spectra were collected with a Shimadzu IRAffinity 1S spectrophotometer in the range of 400–4000 cm^{-1}, using a resolution of 4 cm^{-1} and 20 scans. SEM images of samples were recorded on a S4800-Hitachi microscope. Absorbance spectra were recorded in the 300 to 800 nm wavelength range in a Cary 5000, Varian USA spectrophotometer.

II.5. Photocatalytic activity

Photocatalytic activity was studied at room temperature using a UV lamp (66 W, λ_{max} = 254 nm, manufactured by Medicor, Budapest, Hungary, type BLF-12) as light source. The distance of the liquid surface inside the glass reactor from the UV light source was 20 cm. In each experiment carried out in ultrasonic bath, 7.5 mg of powdered photocatalyst was dispersed in 25 ml of a solution of MB (5x10^{-5} M). A dark phase of 30 min preceded each photodegradation test aimed to evaluate the adsorption capacity of the catalysts towards dyes. Throughout the photocatalytic reaction, the samples were withdrawn at defined time steps (0, 30, 60, 90 and 120 min), centrifuged to separate the catalyst prior to analysis.

III. RESULTS AND DISCUSSION

III.1. Characterization of graphene-Au composites

The Raman spectra of the Gr and Gr-Au are presented in Fig. 1 with the D- and G-band positioned near 1345 and 1576 cm^{-1}, respectively. The D-band is generated by the phonon vibrations from a disordered atomic lattice and the sp^3 orbital of oxygen functionalities, i.e., the impurity-induced elastic scattering. The G-band arises from the sp^2 bonding which includes both conjugated and single bonding in the carbon-based materials. In comparison to the Raman spectrum of Gr, the G bands of Gr-Au were broadened because of the enhanced isolated double bonds and the D bands became outstanding due to the enhanced disorder with graphene-Au.

Fig. 1. Raman spectra of Gr and Gr-Au composites.

The G band of the Gr-Au nanocomposite (1585 cm^{-1}) was obviously upshifted by 9 cm^{-1} with respect to Gr (1576 cm^{-1}), which is consistent with previous research that Au introduced would
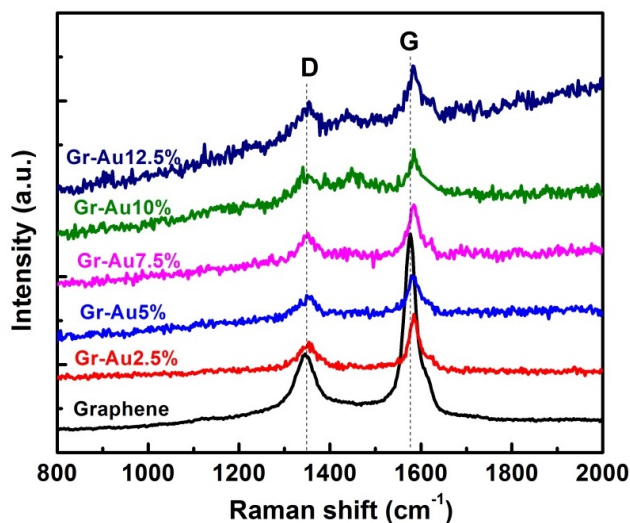
cause upshift of the G band due to the electron–phonon coupling [16]. The intensity ratio of the D to G bands (I_D/I_G) is often used as a measure of defect levels in graphitic systems. With surface modification of Gr sheets with gold NPs, the ratio of I_D/I_G actually increased from 0.4 to 0.62, demonstrating the formation of large sp^3 domain [17]. It was believed that the Au NPs increase the distance between the Gr sheets, thereby making both faces of Gr accessible [18].
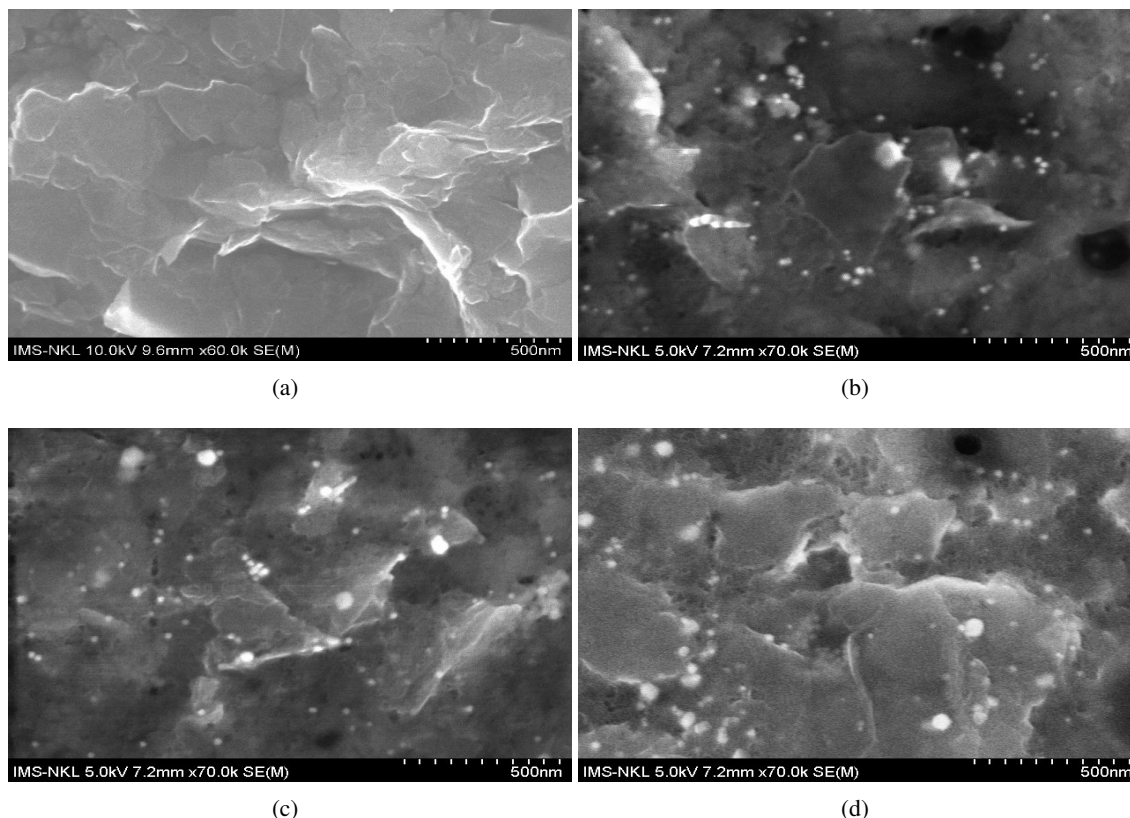

Fig. 2. SEM images of Gr (a), Gr-Au2.5% (b), Gr-Au5% (c) and Gr-Au7.5% (d).

Fig. 2a displays the SEM image of the Gr before impregnation with gold NPs. The SEM image in Fig. 2b-d confirmed that the Au NPs were attached to the surface of the Gr. The white dots in Fig 2b-d are the Au NPs. The size of Au NPs ranges from 10 to 50 nm with an average size of 30 nm.

FTIR spectra of pristine Gr nanoplatelets and Au/Gr have been taken to study the attachment of functional groups (Fig. 3). Noticeable, the additional peaks at 1580 cm^{-1}, 1628 cm^{-1} and 1708 cm^{-1} were attributed to carboxyl or carbonyl groups, and the one at 1175 cm^{-1} was done to C-O bond. It is reported that in the preparation of metal NPs deposited CNTs, functional groups such as carboxyl and carbonyl are responsible for nucleating metal ions, which are reduced to nanosized particles [19].
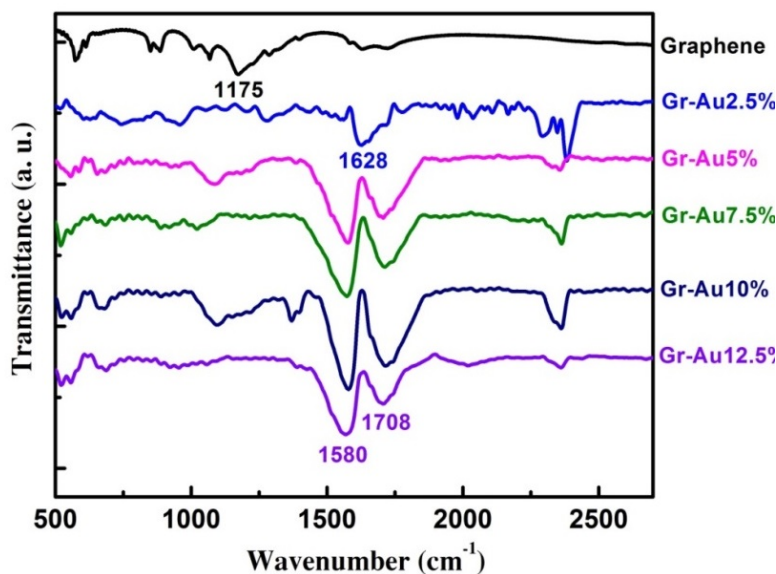
Fig. 3. FTIR spectra for graphene nanoplatelets and graphene-Au.

III.2. Photodegradation of Methylene Blue

The UV light photocatalytic activities of all samples were evaluated by monitoring the degradation of Methylene Blue (MB) dye under UV light ($\sim$ 254 nm) exposure at atmospheric pressure and room temperature. Accordingly, the percentage of dye degradation in terms of C/C_0 was reported. The time dependent degradation of MB dye under exposure of UV light was plotted in Fig. 4a. It was observed from Fig. 4a that MB was degraded efficiently by Gr-TiO_2 to an extent of above 46.5% in 2 h duration, suggesting UV spectrum had effect on the dye degradability. It is noted that TiO_2 could degrade MB to the extent of about 36.7% in UV light. However, for the case of Gr-Au0.1% /TiO_2 and Gr-Au0.15% /TiO_2 composite, they increase about 3.3 fold and 3.1 fold in degradability, respectively (Fig. 4b). Interestingly, the highest rate constant (k) is found for Gr-Au0.1% /TiO_2 sample. Considering the UV light irradiation, the rate constant of Gr-Au0.1% /TiO_2 and Gr-Au0.15% /TiO_2 is very significant for the composite samples.

The photocatalysis process requires the absorption of light to create enough e–h pairs and easy separation of the photoexcited e–h pairs with minimum recombination. In a semiconducting material, the separation of photoexcited e–h pairs with minimum recombination is highly challenging. Efficient separation of the photogenerated e–h pairs is essential for the generation of highly active superoxide and hydroxyl radicals to facilitate redox reaction for the degradation of the dye. On the basis of the above-illustrated enhanced photodegradation under UV light irradiation, the following mechanism can be proposed. A possible band diagram of the Gr-Au/TiO_2 at the interface as well as the carrier transfer mechanism is schematically illustrated in Fig. 5. Previous reports suggest that in the Gr-Au/ZnO, the CB of the ZnO NPs lie above the work function (WF) of the Gr and its of Gr is higher than the one of Au. Therefore, the migration of the photogenerated charge carriers through the interface of these composites is thermodynamically
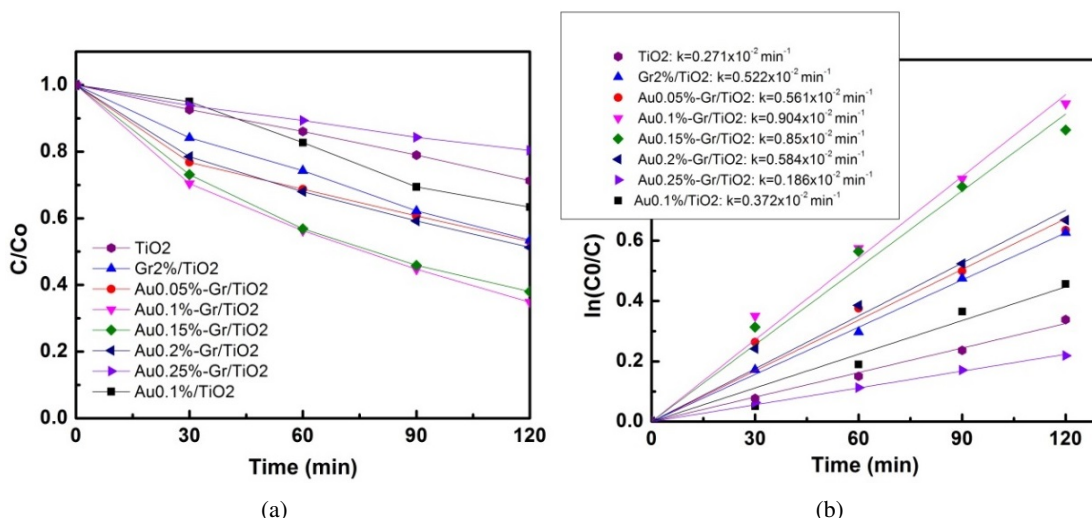
Fig. 4. Normalized rate of removal of MB by samples based on TiO$_2$ under UV light irradiation (a) and kinetic study of the photocatalytic degradation of MB (b).

favorable [20, 21]. The photogenerated electrons and holes react with the adsorbed O$_2$ and H$_2$O molecules, respectively, to form superoxide radicals and hydroxyl radicals. They can degrade most of the organic dyes to the end products. Due to the band positions, photoexcited electrons from the CB of the TiO$_2$ migrate to Gr and then Au. The holes of the VB of the TiO$_2$ still move at this place. Adsorbed O$_2$ and H$_2$O molecules react with the photogenerated electrons at the interface of the heterostructure (HS) to form superoxide radicals, and holes can be trapped by the hydroxyl groups to form hydroxyl radicals. Thus, a sufficient number of powerful super oxide and hydroxyl radicals are generated and they decompose the adsorbed organic pollutants.
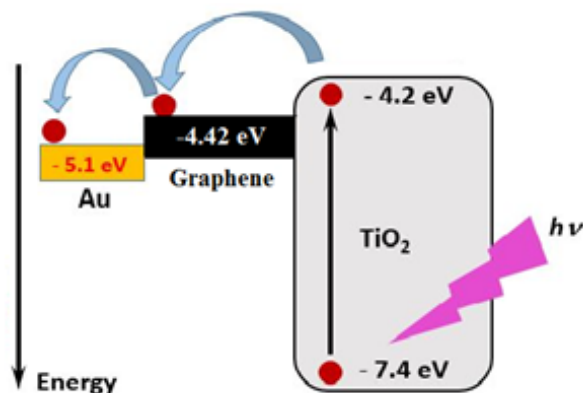

Fig. 5. Schematic diagram showing the electron transfer mechanism from different energy levels of the Graphene-Au/TiO$_2$ heterostructure for the photo-reduction. A similar mechanism was reported by Chinh *et al.* [22].

IV. CONCLUSIONS

Gr-Au/TiO$_2$ nanocomposites have been successfully fabricated at ambient temperature. The morphology, structure, phase and elemental composition of the individual component and the HS have been studied by FESEM, FT-IR, Raman studies helped us to understand the optical properties of the systems. Gr-Au act as an electron receptor to improve the photoactivity of TiO$_2$. The thermodynamically favored band structure of the nanocomposite ensures efficient charge separation, prolonging the lifetime of the photogenerated charge carriers that causes enhanced UV light photodegradation activity. Our results demonstrate that Gr-Au/TiO$_2$ is efficient in the degradation of MB dyes. The photocatalytic efficiency and the degradation rate of Gr2% -Au0.1% /TiO$_2$ are maxima in samples. Thus, semiconductor photocatalysts such as TiO$_2$ and ZnO incorporated with Gr-Au could help to enhance efficient charge transfer at the interface leading to improved UV light photocatalysis. These results are significant for the environmental applications.

REFERENCES

[1] M. A. Shannon, P. W. Bohn, M. Elimelech, J. G. Georgiadis, B. J. Marinas, and A. M. Mayes, *Nature* **452** (2008) 301.

[2] K. Rajeshwar, M. E. Osugi, W. Chanmanee, C. R. Chenthamarakshan, M. V. B. Zanoni, P. Kajitvichyanukul, and R. Krishnan-Ayer, *J. Photochem. Photobiol. C: Photochem. Rev.* **9** (2008) 15.

[3] A. Fujishima, X. Zhang, and D.A. Tryk, *Surf. Sci. Rep.* **63** (2008) 515–582.

[4] J. Shen, M. Shi, N. Li, B. Yan, H. Ma, Y. Hu, and M. Ye, *Nano Res.* **3** (5) (2010) 339-349.

[5] X. Zhou, X. Huang, X. Qi, S. Wu, C. Xue, F. Y. C. Boey, Q. Yan, P. Chen, and H. Zhang, *J. Phys. Chem. C* **113** (2009) 10842.

[6] K. Jasuja and V. Berry, *ACS Nano* **3** (8) (2009) 2358.

[7] H. Yin, H. Tang, D. Wang, Y. Gao, and Z. Tang, *ACS Nano* **6** (2012) 8288.

[8] C. Xu, X. Wang, and J. Zhu, *J. Phys. Chem. C* **112** (2008) 19841.

[9] P. V. Kamat, *J. Phys. Chem. Lett.***1** (2)(2010) 520.

[10] G. Williams and P. V. Kamat, *Langmuir* **25** (2009) 13869.

[11] Y. Wang, S. Zhang, D. Du, Y. Y. Shao, Z. H. Li, J. Wang, M. H. Engelhard, J. H. Li, and Y. H. Lin, *J. Mater. Chem.***21** (2011) 5319.

[12] D. Xiaochen, H. Wei, and C. Peng, *Nanoscale Res. Lett.* **60** (2011) 1.

[13] G. Goncalves, P. A. A. P. Marques, C. M. Granadeiro, H. I. S. Nogueira, M. K. Singh, and J. Gracio, *Chem. Mater.* **21** (2009) 4796.

[14] P. A. Pandey, G. R. Bell, J. P. Rourke, A. M. Sanchez, M. D. Elkin, B. J. Hickey, and N. R. Wilson, *Small* **7** (2011) 3202.

[15] J. Li, C. Y. Liu, and Y. Liu, *J. Mater. Chem.* **22** (2012) 8426.

[16] H. Zhang, S. Chen, X. Quan, H. T. Yu, and H. M. Zhao, *J. Mater. Chem.* **21** (2011) 12986.

[17] V. Singh, D. Joung, L. Zhai, S. Das, S. I. Khondaker, and S. Seal, *Prog. Mater. Sci.* **56** (2011) 1178.

[18] Y. Si and E. T. Samulski, *Chem. Mater.* **20** (2008) 6792.

[19] W. Li, C. Liang, W. Zhou, J. Qiu, G. Zhou, Q. Sun, and J. Xin, *Phys. Chem. B* **107** (2003) 6292.

[20] N. T. Khoa, S. W. Kim, D. H.Yoo, S. Cho, E. J. Kim, and S. H. Hahn, *ACS Appl. Mater. Interfaces* **7** (2015) 3524.

[21] P. Roy, A. P.Periasamy, C-T. Liang, and H-T. Chang, *Environ. Sci. Technol.* **47** (2013) 6688.

[22] V. D. Chinh, L. X. Hung, L. Di Palma, V. T. H. Hanh and G. Vilardi, *Chem. Eng. Technol.* **42** (2019) 308.